ACS APPLIED MATERIALS & INTERFACES

RESEARCH ARTICLE

www.acsami.org

Self-Healing Epoxy Composite with Heat-Resistant Healant

Yan Chao Yuan,[†,‡] Xiao Ji Ye,[§] Min Zhi Rong,[§] Ming Qiu Zhang,[*,§] Gui Cheng Yang,[§] and Jian Qing Zhao[†]

[†]College of Materials Science and Engineering, South China University of Technology, Guangzhou 510640, P. R. China

[‡]Key Laboratory for Polymeric Composite and Functional Materials of Ministry of Education, DSAPM Lab, School of Chemistry and Chemical Engineering, and [§]Materials Science Institute, Sun Yat-sen (Zhongshan) University, Guangzhou 510275, P. R. China

Supporting Information

ABSTRACT: To provide self-healing epoxy composite with adequate heat resistance for high-performance application, we developed a novel microencapsulated epoxy/mercaptan healing agent. The key measure lies in usage of diglycidyl ether of bisphenol A (EPON 828) as the polymerizable component and 2,4,6-tris(dimethylaminomethyl)phenol (DMP-30) as the catalyst. Because of the higher thermal stability of EPON 828 and lower volatility of DMP-30, the healing agent and the self-healing composite not only survive high-temperature curing and thermal exposure, but also offer satisfactory capability of autonomous properties restoration, as characterized by both fracture mechanics and fatigue tests. Especially when the operation temperature is not higher than 200 °C, the performance of the healing system is nearly independent of thermal history.

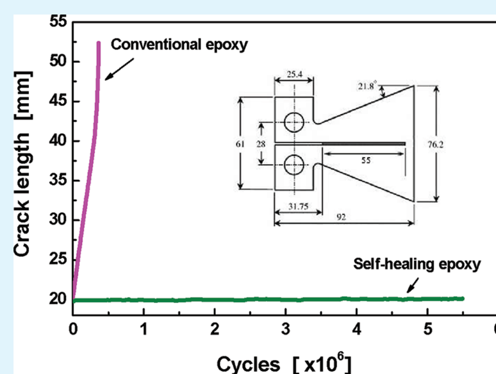

KEYWORDS: self-healing, thermal stability, high-temperature cured epoxy composites, fracture, fatigue

1. INTRODUCTION

Recently, more and more materials scientists have devoted their attention to the development of self-healing polymers and polymer composites.[1−3] Compared to intrinsic self-healing materials that operate based on remendability of macromolecules themselves, extrinsic self-healing is determined by the performance of embedded healing agent.[3] In this context, healing agent with adequate heat resistance is necessary for (i) manufacturing of high-performance composites that require elevated processing temperature and (ii) application in intermittent or continuous high-temperature environment that used to be encountered in practice. To the best knowledge of the authors, however, research in this direction has not yet been widely conducted.[4−16]

Among the few available literature reports, Mangun and co-workers[17] incorporated microcapsules respectively containing poly(dimethylsiloxane) (PDMS) and organotin catalyst into epoxy, and evaluated self-healing ability of the composite that had been treated at 177 °C for 4 h. Jin et al.[18] developed a dual-microcapsule epoxy-amine based self-healing system for use in high temperature cured epoxy.

In the authors' lab, self-healing epoxy composites with dual encapsulated epoxy/mercaptan healant were prepared. Epoxy prepolymer (diglycidyl tetrahydro-o-phthalate, DTP) plays the role of polymerizable resin, while the mixture of mercaptan (pentaerythritol tetrakis (3-mercaptopropionate), PMP) and tertiary amine catalyst (benzyl dimethylamine, BDMA) acts as the hardener.[19−21] The system proved to work as characterized by attractive room temperature healing effect even when the composites were stored at 120 °C for 12 h. Nevertheless, a further rise in environmental temperature greatly deteriorates the healing performance. When the composites were exposed to 150 °C for 12 h, for example, the healing efficiency dropped from 104 to 35%. Thermal degradation of the epoxy prepolymer[19] and leakage of the highly volatile amine[18] should take the responsibility. Considering that the mercaptan used in the self-healing system has higher thermal stability than the rest two components (i.e., epoxy prepolymer and tertiary amine catalyst), replacement of the latter with more robust versions (i.e., diglycidyl ether of bisphenol A (EPON 828) and 2,4,6-tris(dimethylaminomethyl)-phenol (DMP-30)) would be a possible solution without the expenses of healing ability. In the meantime, curing mechanism of the healing system would remain unchanged.

Accordingly, the objective of this work is to verify the above idea in terms of both fracture toughness and fatigue tests. It is hoped that heat resistance of the healing agent can thus be enhanced, broadening application coverage of the self-healing epoxy composites.

2. EXPERIMENTAL SECTION

2.1. Materials and Specimens Preparation. The encapsulated healing agent (i.e., epoxy prepolymer and its hardener) was made by using poly(melamine-formaldehyde) (PMF) as the microcapsule shell according to the method described elsewhere.[19,20] The epoxy-loaded microcapsules hold diglycidyl ether of bisphenol A (EPON 828, Hexion Specialty Chemicals), while the hardener-loaded microcapsules include pentaerythritol tetrakis (3-mercaptopropionate) (PMP, Fluka Chemie AG)

Received: September 1, 2011
Accepted: October 12, 2011
Published: October 12, 2011

ACS Publications © 2011 American Chemical Society

Table 1. Description of the Microencapsulated Healing Agent

name	average diameter (μm)	density (g/cm^3)	core substance	
			ingredient	content (wt %)
epoxy-loaded microcapsules	103.9	1.26	EPON 828	97.1
hardener-loaded microcapsules	102.1	1.23	PMP	81.2
			DMP-30	15.7
polythiol-loaded microcapsules	101.9	1.25	PMP	97.1

Table 2. Properties of the Specimens of Cured Epoxy and Its Composites

property	neat epoxy specimens	control specimens[a]	specimens with healing capsules[b]
density (g/cm^3)	1.175	1.183	1.189
K_{IC} (MPa m$^{1/2}$)	0.583 ± 0.021	0.698 ± 0.034	0.702 ± 0.037
Young's modulus (GPa)	3.7 ± 0.2	3.2 ± 0.1	3.2 ± 0.1

[a] The control specimens are made from room temperature curing system and contain 10 wt % epoxy-loaded microcapsules and 10 wt % polythiol-loaded microcapsules (excluding tertiary amine catalyst). [b] The specimens with healing capsules are made from room temperature curing system and contain 10 wt % epoxy-loaded microcapsules and 10 wt % hardener-loaded microcapsules.

and 2,4,6-tris(dimethylaminomethyl)phenol (DMP-30, Shanghai Medical Group Reagent Co., China). For comparative study, polythiol-loaded microcapsules containing only PMP without amine catalyst were also synthesized. Because epoxy prepolymer can only be cured within reasonable time span by mercaptan in the presence of tertiary amine, the mixture of released fluids from epoxy- and polythiol-loaded microcapsules would not be timely polymerized. That is, the paired epoxy- and polythiol-loaded microcapsules in epoxy composite would hardly offer any healing effect under the conventional test conditions.[20] Table 1 lists the specifications of the microcapsules.

The specimens of epoxy and its composites filled with encapsulated healing agent were made by means of room temperature curing system, medium temperature curing system and high temperature curing system, respectively. The details are given in the following.

In the case of room-temperature curing system, unfilled epoxy specimens in the form of tapered double cantilever beam (TDCB, with groove length of 55 mm[20,22]) were cast from the mixture of 100 parts EPON 828 and 12.5 parts diethylenetriamine (DETA, Shanghai Medical Group Reagent Co., China), whereas the self-healing epoxy specimens of the same configuration were prepared by uniformly mixing 10 wt % epoxy-loaded microcapsules and 10 wt % hardener-loaded microcapsules with the aforesaid mixture of EPON 828 and DETA. Control specimens were fabricated with addition of 10 wt % epoxy-loaded microcapsules and 10 wt % polythiol-loaded microcapsules (that exclude tertiary amine catalyst). The compounds were degassed, poured into a closed silicone rubber mold and cured for 24 h at room temperature, followed by 48 h at 40 °C. Table 2 shows properties of the specimens.

As for the medium-temperature curing system, 2-ethyl-4-methylimidazole (2E4MIm, Shanghai Medical Group Reagent Co., China) was employed as curing agent of the matrix. Unfilled epoxy specimens in the form of TDCB were cast from the mixture of 100 parts EPON 828 and 2 parts 2E4MIm, while the self-healing epoxy specimens of the same configuration were prepared by uniformly mixing 10 wt % epoxy-loaded microcapsules and 10 wt % hardener-loaded microcapsules with the aforesaid mixture of EPON 828 and 2E4MIm. The compounds were degassed, poured into a preheated closed silicone rubber mold, and cured at 80 °C for 2 h, 120 °C for 2 h, and 140 °C for 2 h.

With respect to the high-temperature curing system, 4,4-diaminodiphenysulfone (DDS, Shanghai Medical Group Reagent Co., China) was employed as curing agent of the matrix. 100 parts EPON 828 was heated to 120 °C and 32 parts DDS was added under continuous stirring. The mixture was kept at 120 °C for about 1 h to dissolve the incorporated DDS. Unfilled epoxy specimens in the form of TDCB were cast from the mixture, whereas the self-healing epoxy specimens of the same configuration were prepared by uniformly mixing 10 wt % epoxy-loaded microcapsules and 10 wt % hardener-loaded microcapsules with the aforesaid mixture of EPON 828 and DDS. The compounds were degassed, poured into a preheated closed silicone rubber mold and cured at 100 °C for 3 h, 140 °C for 2 h, and 180 °C for 4 h.

2.2. Thermal Exposure. To evaluate heat resistance of the encapsulated healing agent and self-healing epoxy composite, we heated the above self-healing and control specimens in an oven at different temperatures (50−300 °C) for different times (0−24 h).

2.3. Characterization. Thermogravimetric analyses (TGA) of the microcapsules were carried out using Netzsch TG-209 instrument. The samples were heated from 25 to 600 °C at a rate of 10 °C/min under the protection of nitrogen flow. In-situ microinfrared spectra were recorded with a Bruker EQUINOX55 Fourier transformation infrared spectrometer coupled with a HYPERION™ A670-B infrared microscope spectrometer and a high-resolution digital camera. Morphological observation and energy dispersive spectroscopy (EDS) analysis were conducted by a HITACHI model S-4800 field emission scanning electron microscope (SEM). Prior to the experiment, the specimen surface was coated by gold/palladium sputter.

To quantify fracture toughness and development of healing efficiency of the epoxy specimens, we created a precrack (∼2.5 mm) on the TDCB specimens by inserting a fresh razor blade and gently tapping into the molded notch starter.[20] Subsequently, the specimen was pin loaded and tested with a Hounsfield 10K−S universal testing machine under displacement control using a 0.3 mm/min displacement rate at room temperature (24 ± 1 °C). Specimens were fractured only to the end of the groove. For specimens with healing capsules, they were unloaded, allowing the crack faces to come back into contact and to be self-healed at certain temperature in an incubator for different times. Finally, the healed specimens were tested again following the above procedure. Efficiency of healing, η, was calculated from the ratio of fracture toughness, K_{IC}, of healed (i.e., K_{IC}^{Healed}) and virgin (i.e., K_{IC}^{Virgin}) materials:[4,22]

$$\eta = \frac{K_{IC}^{Healed}}{K_{IC}^{Virgin}} \times 100\%$$

Each batch included six specimens to yield averaged value. More details of the measurement are available in ref 19.

Fatigue crack propagation behavior of the TDCB specimens was studied by a Shimadzu air servo fatigue and endurance testing system ADT-AV02K1S5 with 2 kN load cell at room temperature (24 ± 1 °C). The specimens were precracked (∼2.5 mm) with a razor blade while ensuring the precrack tip was centered in the groove and immediately cyclically loaded. A triangular waveform of frequency 5 Hz was applied with a stress ratio, R, of 0.1 ($R = K_{min}/K_{max}$, where K_{min} and K_{max} denote the minimum and maximum values of the cyclic stress intensity, respectively). Fatigue cracks were grown within constant mode-I stress intensity factor range, ΔK_I ($\Delta K_I = K_{max} - K_{min}$). Load line crack opening displacement (COD) was measured by a clip gauge. Mode I fatigue cracks were constrained along the centerline of the specimen because of use of side grooves molded in the specimen. The optically

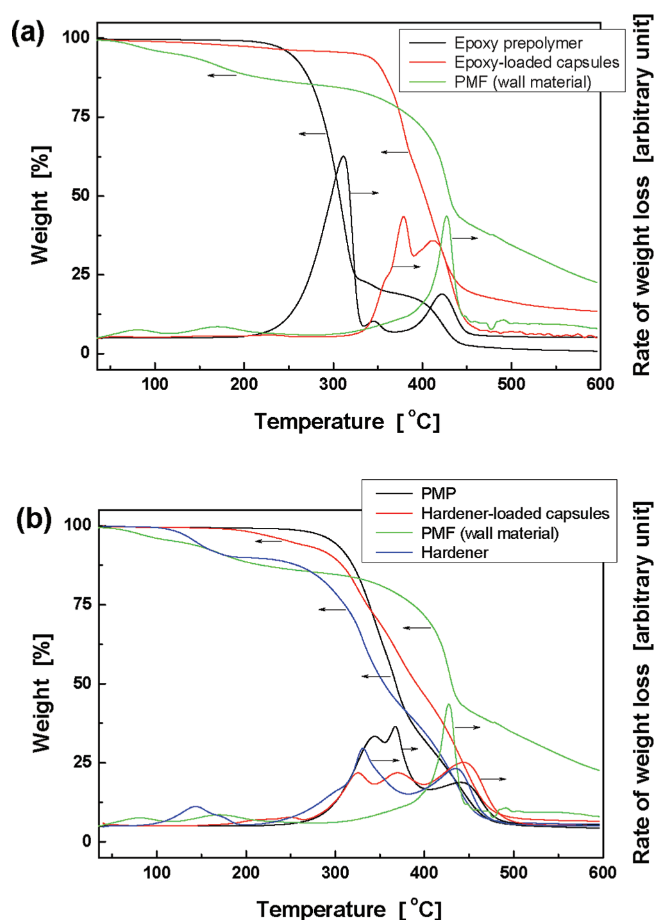

Figure 1. Thermogravimetric analysis of microencapsulated healing agent. The hardener in (b) refers to the mixture of 83.8 wt % PMP and 16.2 wt % DMP-30.

measured crack tip position and specimen compliance were plotted against number of cycles. The linear relationship between optically measured crack length and specimen compliance was used to calculate the crack tip position of the specimens at all times during the experiment.[23,24] Healing efficiency, λ, was defined by fatigue life extension[24,25]

$$\lambda = \frac{N_{\text{Healed}} - N_{\text{Control}}}{N_{\text{Control}}} \times 100\%$$

where N_{Healed} and N_{Control} denote the total number of cycles to failure of the healed specimen and that of a similar control specimen without healing, respectively. For each test, the result was an average of five specimens.

3. RESULTS AND DISCUSSION

3.1. Thermal Stability and Durability of Microencapsulated Healing Agent. Prior to evaluation of influence of thermal exposure on healing ability of the composites, thermal stability of the microencapsulated healing agent should be known. By using thermogravimetric analysis, it is seen that no detectable change in the epoxy prepolymer EPON 828 is found when temperature is lower than 200 °C (Figure 1a). With respect to encapsulated EPON 828, the thermal stability is significantly improved, as characterized by an increase of onset temperature of more than 130 °C. In addition, morphology of the epoxy-loaded microcapsule nearly does not change in the course of heating from room temperature to 300 °C (Figure 2a−d). The isothermal experiment at 200 °C indicates that the weight loss rapidly reaches 1.92 wt % within 2 h and then slowly increases to 2.76 wt % after 24 h (Figure 3a). It should be due to evaporation of the adsorbed water and formaldehyde from deformaldehyde reaction of PMF at elevated temperature.[26] On the whole, the epoxy-loaded microcapsules have good closure and heat resistance.

Pyrolytic analysis of polythiol PMP demonstrates that its onset temperature is about 250 °C (Figure 1b). In contrast, tertiary amine catalyst DMP-30 is volatilized from the hardener (i.e., mixture of 83.8 wt % PMP and 16.2 wt % DMP-30) between 100 to 200 °C. When the hardener is encapsulated, however, its thermal stability is improved as expected. Morphology of the hardener-loaded microcapsule also keeps unchanged during heating up to 300 °C (Figure 2e−h). The isothermal thermogravimetric analysis at 200 °C shows that weight loss of the hardener-loaded microcapsules is only 2.13 wt % after 24 h (Figure 3a), as a result of evaporation of the adsorbed water, trace amount of DMP-30 and formaldehyde from the deformaldehyde reaction of PMF at elevated temperature.[26] Clearly, the hardener-loaded microcapsules are accompanied with reasonably high thermal stability like the epoxy-loaded counterparts.

On the other hand, the microencapsulated healing agent possesses long-term durability even after being exposed to high temperature (e.g., 200 °C for 24 h). Figure 3b shows that the additional weight losses of the epoxy- and hardener-loaded microcapsules at room temperature for 11 months are only about 0.013 and 0.018 wt %, respectively. Visual inspection does not find the microcapsules stick together and their appearances also remain unchanged after long time storage. Because the microcapsules are embedded in epoxy matrix in practical usage, the results in Figure 3 evidence that thermal stability and durability of self-healing capability of the composites must have been obviously improved, as compared with the original system containing DTP and BDMA (refer to the Introduction).

To further understand whether the functional groups of the healing agent remain their reactivity after being exposed to high temperature, we first heated the epoxy- and hardener-loaded microcapsules to different temperatures (200−250 °C) for 24 h. Having been placed at room temperature for over 24 h, they were crushed on quartz glasses and analyzed by micro-IR spectroscopy (Figures 4 and 5), respectively.

It is seen from Figure 4 that characteristic stretching peaks of epoxide group at 915 cm^{-1} and O−H group at 3413 cm^{-1} appear on the FTIR spectra, representing the existence of epoxy prepolymer. The spectrum profiles and peak positions are the same after high temperature exposure. By using the peak area of inert C−H group from 3087 to 2814 cm^{-1} as the reference, the peak area ratio of epoxide group/O−H group/C−H group on the core material spectrum of the capsules exposed to 200 °C for 24 h is estimated to be 0.213/0.650/1 (curve b in Figure 4). The value is almost identical to the result of raw epoxy prepolymer (0.216/0.649/1, curve a in Figure 4), suggesting that the core material in epoxy-loaded capsules has no variation. When the epoxy-loaded microcapsules are exposed to 225 and 250 °C for 24 h, however, the FTIR peak area ratios of epoxide group/O−H group/C−H group become 0.208/0.652/1 (curve c in Figure 4) and 0.202/0.644/1 (curve d in Figure 4), respectively. It means that the epoxy prepolymer has been slightly degraded, despite the fact that nearly no loss in weight is perceived (Figure 1a).

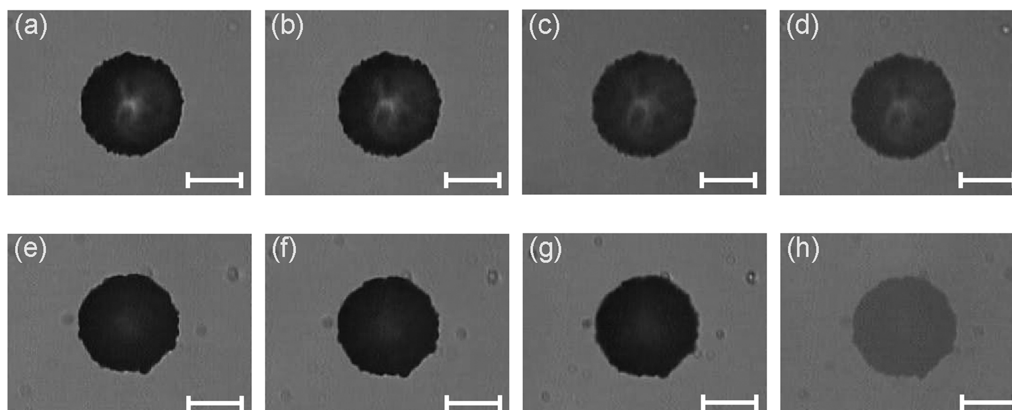

Figure 2. Micrographs of (a−d) a representative epoxy-loaded microcapsule and (e−h) hardener-loaded microcapsule at different temperatures. (a, e) 30, (b, f) 100, (c, g) 200, and (d, h) 300 °C. The attached scale bars represent 60 μm in length. Rate of heating: 1 °C/min.

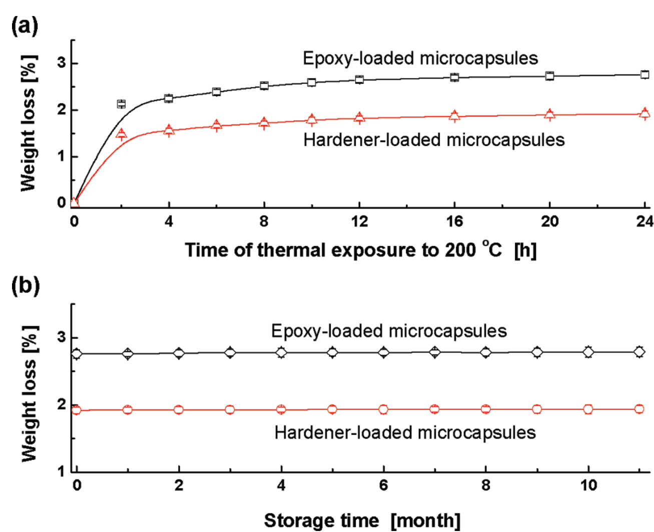

Figure 3. Effects of high-temperature exposure time and storage time on stability of epoxy-loaded and hardener-loaded microcapsules. (a) Weight loss of the microcapsules as a function of exposure time at 200 °C. (b) Weight loss of the microcapsules as a function of storage time at room temperature. For b, the microcapsules had been heat treated at 200 °C for 24 h in advance, so that the initial data of weight loss (at time = 0) are equal to the weight loss at 24 h in a.

The FTIR spectra in Figure 5 reveal characteristic stretching peaks of S−H group from PMP at 2568 cm^{-1} and benzene ring from DMP-30 at 1611 cm^{-1}. The high temperature exposure does not result in any variation in chemical structures of the substances, as either the spectrum profiles or peak positions are the same after the high temperature exposure. When the peak area of inert C−H group from 3048 to 2736 cm^{-1} serves as the reference, the peak area ratio of S−H group/benzene ring/C−H group on the core material spectrum of the hardener-loaded microcapsules exposed to 200 °C for 24 h is estimated to be 0.142/0.070/1 (curve b in Figure 5). It is close to the value of the original hardener (0.143/0.062/1, curve a in Figure 5). It manifests that the main ingredient of the core material of hardener-loaded capsules, PMP, remains unchanged, but the minor constituent DMP-30 is marginally volatilized off. In the case of higher exposure temperature (i.e., 225 and 250 °C),

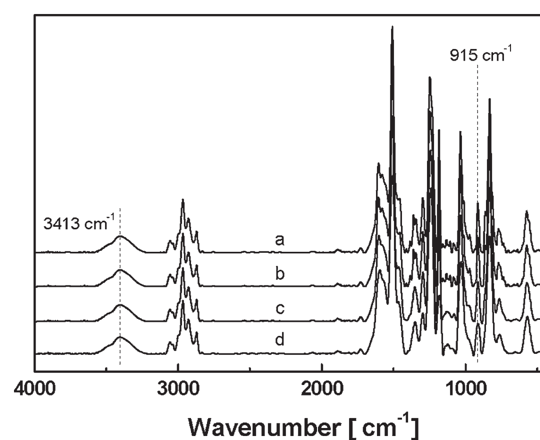

Figure 4. In situ micro-IR spectra of the core substance released from epoxy-loaded microcapsules that had been exposed to 200 °C for 24 h. High-temperature exposure history of the microcapsules: (a) no high-temperature exposure; (b) 200 °C, 24 h; (c) 225 °C, 24 h; (d) 250 °C, 24 h.

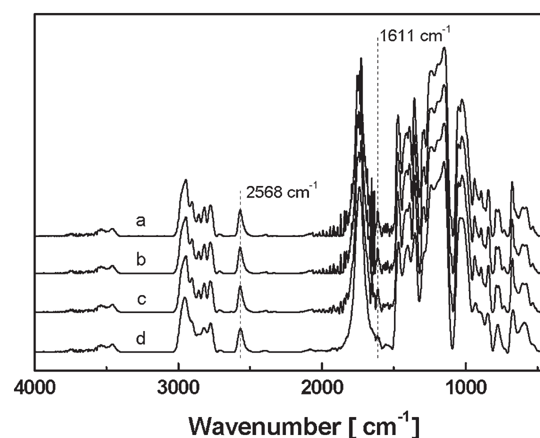

Figure 5. In situ micro-IR spectra of the core substance released from hardener-loaded microcapsules that had been exposed to 200 °C for 24 h. High-temperature exposure history of the microcapsules: (a) no high-temperature exposure; (b) 200 °C, 24 h; (c) 225 °C, 24 h; (d) 250 °C, 24 h.

the peak area ratios of S−H group/benzene ring/C−H group are 0.141/0.041/1 (curve c in Figure 5) and 0.140/0.031/1

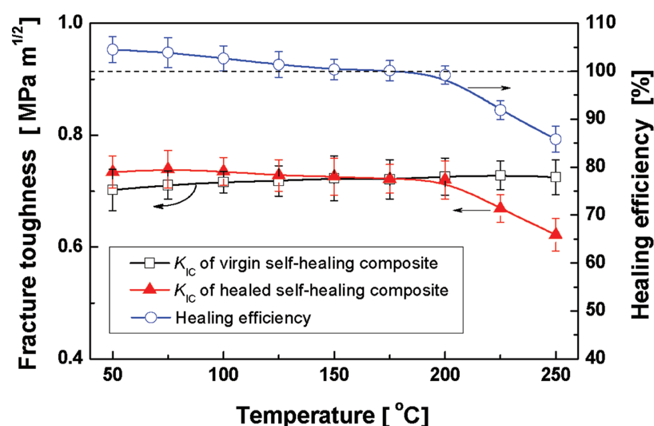

Figure 6. Influence of thermal exposure temperature on healing efficiency. The specimens with healing capsules made from room temperature curing system were first exposed to different temperatures for 24 h. Having been placed at room temperature for more than 24 h, they were measured by the standard fracture toughness test procedure. Healing of the fractured specimens was conducted at room temperature for 24 h.

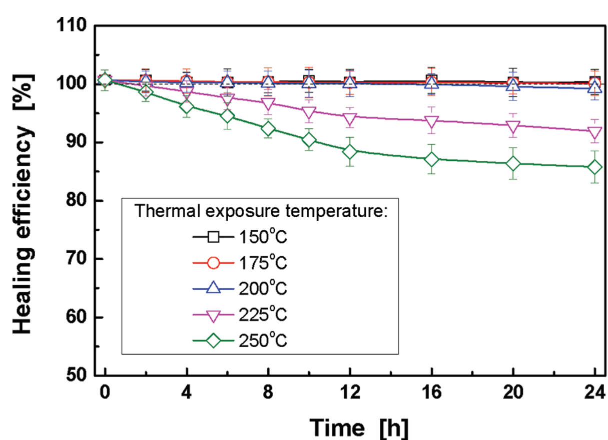

Figure 7. Influence of thermal exposure time on healing efficiency. The specimens with healing capsules made from room temperature curing system were first exposed to different temperatures for 24 h. Having been placed at room temperature for more than 24 h, they were measured by the standard fracture toughness test procedure. Healing of the fractured specimens was conducted at room temperature for 24 h.

(curve d in Figure 5), respectively. The results indicate that PMP is hardly degraded under the circumstances, while 31.9 and 51.5 wt % DMP-30 are volatilized off, respectively. This would certainly affect consolidation of the released healing agent in the course of crack healing.

3.2. Effect of Thermal Exposure on Healing Ability Studied by Monotonic Fracture Tests. The influence of thermal exposure on healing efficiency is shown in Figures 6 and 7 in terms of fracture toughness recovery. The specimens with healing capsules were first exposed to different temperatures for different times. Having been placed at room temperature for over 24 h, they were measured by the standard fracture toughness test procedure. The results exhibit that the exposure temperature between 50 and 250 °C has little impact on fracture toughness of the virgin composites, but obviously brings down fracture toughness of the healed composites, especially when temperature exceeds 200 °C (Figure 6). Accordingly, healing efficiency mildly declines before 200 °C, and the down tendency becomes apparent as of 200 °C. Moreover, longer exposure time at temperatures higher than 200 °C corresponds to lower healing efficiency (Figure 7). When the specimens are exposed to 250 °C for 24 h, for example, the healing efficiency is decreased to 85.8%. In contrast, healing efficiency is nearly independent of exposure time when the specimens are exposed to temperatures lower than 200 °C.

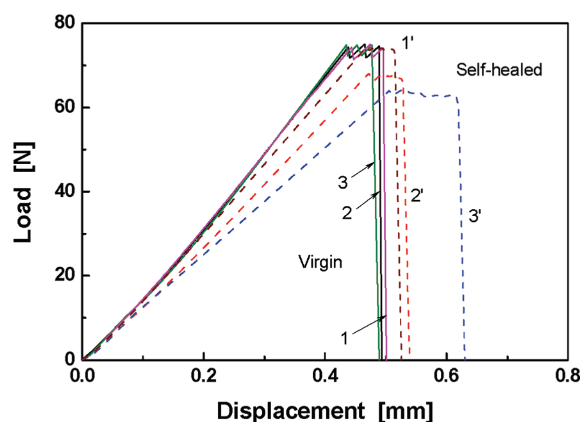

Figure 8. Typical load−displacement curves recorded during TDCB tests. The specimens with healing capsules made from room temperature curing system were first exposed to 200 °C for 24 h (curves 1 and 1′), 225 °C (curves 2 and 2′), and 250 °C (curves 3 and 3′), respectively. Having been placed at room temperature for over 24 h, they were measured by the standard fracture toughness test procedure. Healing of the fractured specimens was conducted at room temperature for 24 h.

Certainly, these phenomena are related to heat resistance of the encapsulated healing agent. As revealed above, epoxy- and hardener-loaded microcapsules developed in this work can be long-time handled at temperatures no higher than 200 °C without significant deterioration. Therefore, the thermal exposure at temperatures lower than 200 °C only marginally reduces fracture toughness and healing efficiency of the healed composites. In the case of higher temperature exposure, slight partial thermal degradation of the epoxy prepolymer and leakage of DMP-30 catalyst occur, which might decrease curing rate and cross-linking degree of the released healing agent.

Figure 8 shows typical load−displacement curves of the specimens with healing capsules recorded during TDCB tests. The compliances of virgin specimens before crack propagation, which had been exposed to different temperatures for 24 h, are 5.763 μm/N (curve 1), 5.805 μm/N (curve 2) and 5.562 μm/N (curve 3), respectively. Comparatively, the values of healed specimens are increased to 6.111 μm/N (curve 1′), 6.822 μm/N (curve 2′) and 7.857 μm/N (curve 3′), respectively. The results support the above analysis that higher exposure temperature (200−250 °C) leads to lower curing degree of the released healing agent. Meanwhile, fracture mode turns from corporate cohesive failure of matrix and cured epoxy membrane (see the Supporting Information Figure S1a) to cohesive failure of cured epoxy membrane (see the Supporting Information Figure S1b,c).[19,20]

Figure 9 collects the results of crack healing at different temperatures in the specimens with healing capsules that had been exposed to 200 °C for 12 h. It is seen that healing is very fast at temperatures from 10 to 30 °C. The healing efficiency attains 80−87% after 3 h at 20 and 30 °C, and exceeds 100% only after 12 h.

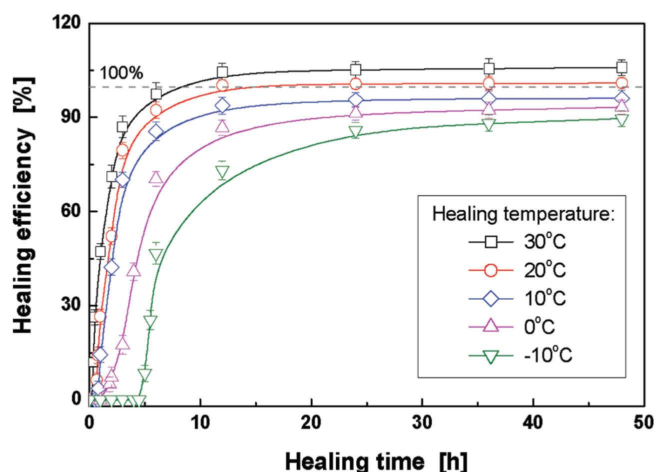

Figure 9. Time dependence of healing efficiency at different temperatures. The specimens with healing capsules made from room temperature curing system were exposed to 200 °C for 12 h in advance. Having been placed at room temperature for over 24 h, they were measured by the standard fracture toughness test procedure. Healing of the fractured specimens was conducted at different temperatures for different times.

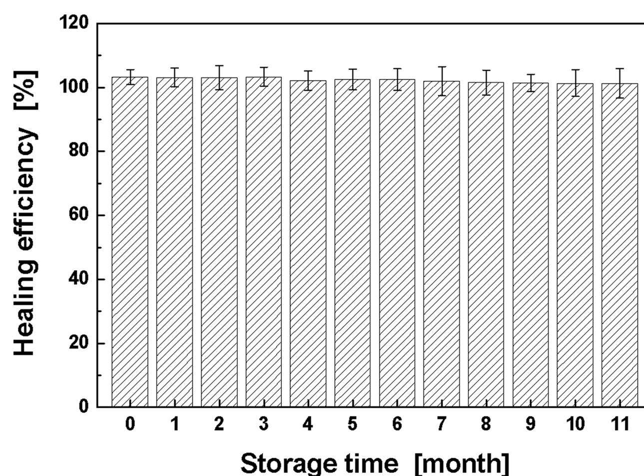

Figure 10. Healing efficiency of the self-healing epoxy composites stored at room temperature for different times. All the specimens were made from room temperature curing system and exposed to 200 °C for 12 h in advance. Healing of the fractured specimens was conducted at room temperature for 24 h.

Although the self-repair process is slowed with decreasing healing temperature, an 88% recovery at −10 °C is observed after 36 h. The results resemble those of the specimens with microencapsulated healant consisting of DTP, PMP and BDMA,[19] which has poor heat resistance.

To characterize long-term durability of the self-healing composites after thermal exposure, healing efficiency of the specimens exposed to 200 °C for 12 h was determined as a function of room temperature storage time. The data in Figure 10 demonstrate that no deterioration is detected within 11 months, which coincides with the durability of the microencapsulated healing agent (Figure 3(b)).

In sum, excessively high temperature exposure would remarkably reduce healing effect of the present self-healing epoxy composites. As long as exposure temperature is not higher than 200 °C, self-healing performance of the composites approaches to that without experiencing thermal exposure.

3.3. Effect of Thermal Exposure on Healing Ability Studied by Fatigue Tests. Dynamic self-healing ability of the composites with high temperature exposure is evaluated by fatigue tests in this subsection. Table 2 shows that the presence of 20 wt % microcapsules (i.e., 10 wt % epoxy-loaded microcapsules and 10 wt % polythiol-loaded microcapsules or hardener-loaded microcapsules) has raised the virgin monotonic fracture toughness of epoxy by up to ∼20%. The toughening effect is not influenced by the thermal exposure (200 °C, 12 h), and improves the composites' fatigue performance because of the increased resistance to fatigue crack propagation (cf. curves a and b in Figure 11). Accordingly, fatigue fracture morphology is changed from mirrorlike one of the unfilled epoxy to hackle markings of the capsules filled versions (see the Supporting Information, Figure S2). The result coincides with previous reports on similar systems, where crack pinning mechanism was believed to take the responsibility.[19,22,27]

Because the competition between polymerization kinetics and crack growth is a major factor affecting successful healing, various levels of applied range of stress intensity were prescribed for the fatigue tests of specimens with healing capsules hereinafter: high

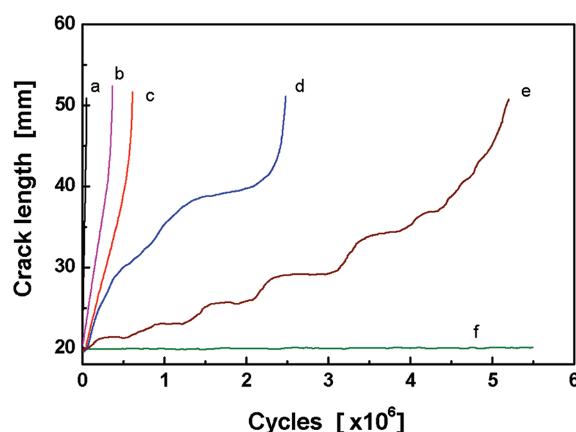

Figure 11. Crack length vs fatigue cycle of (a) neat epoxy specimen with ΔK_I = 0.514 MPa m$^{1/2}$, (b) control specimen with ΔK_I = 0.514 MPa m$^{1/2}$, (c) specimen containing healing capsules with ΔK_I = 0.605 MPa m$^{1/2}$, (d) specimen containing healing capsules with ΔK_I = 0.554 MPa m$^{1/2}$, (e) specimen containing healing capsules with ΔK_I = 0.529 MPa m$^{1/2}$, and (f) specimen containing healing capsules with ΔK_I = 0.514 MPa m$^{1/2}$. For all the tests, R = 0.1, f = 5 Hz. All the specimens were made from room-temperature curing system and exposed to 200 °C for 12 h in advance. Having been placed at room temperature for more than 24 h, they were tested under cyclic loading.

and low cycle fatigue cases.[23,24] The high cycle fatigue refers to the fatigue regime of low ΔK_I, relatively slow crack growth rate and longer fatigue life (even infinite life). Low cycle fatigue refers to the fatigue regime where K_{max} approaches K_{IC}, and rapid crack growth causes specimen failure after very short time.

In the case of low ΔK_I, chemical kinetics of the healing agent plays the leading role. Crack can be fully arrested within short time if the healing system works well, and hence infinite fatigue life extension is obtained. In this regime, the specimen's fatigue life exceeds the time for the healing agent to gel and for quasi-static healing efficiency to develop.[24] As shown by curve f in Figure 11, where ΔK_I = 0.514 MPa m$^{1/2}$ (K_{max}/K_{IC} = 0.79), the

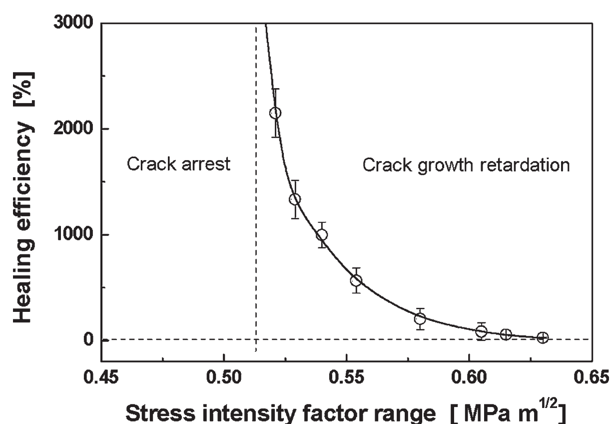

Figure 12. Healing efficiency of specimens with healing capsules as a function of stress intensity factor range, ΔK_I. The data are calculated partly using the results of Figure 11.

specimen with healing capsules was precracked and immediately cyclically loaded. The initial release of healing agent during precracking first retards the crack growth, and leads to certain amount of crack regression (~ 2 mm). After a few cycles, the crack does not further progress within the time frame of the test (~1×10^7 cycles) and is fully arrested. It means that the healing efficiency is infinite. This behavior was repeatedly observed for all the five specimens tested. In contrast, the precrack in the control specimen is more rapidly growing at a constant rate (see curve b in Figure 11).

When the specimen containing healing capsules with fully arrested fatigue crack was fractured under static load without precrack, its fracture toughness was found to be 0.987 MPa $m^{1/2}$, which is much higher than that of virgin specimen with healing capsules (0.723 MPa $m^{1/2}$). As shown in the Supporting Information, Figure S2i,k, the healing agent released during precracking has formed a partial polymer wedge at the crack tip. Corporate cohesive failure of matrix and cured healing agent is confirmed by SEM (see the Supporting Information, Figure S2k), micro-Raman and energy dispersive spectroscopy (EDS) analysis (figure omitted). It implies that stronger adhesion effect is obtained under the circumstances of lower ΔK_I, which favors arresting fatigue crack. Therefore, adhesive bonding and polymeric wedge shielding mechanisms play an important role to indefinitely extend fatigue life of the material in this regime.

With a slight rise in ΔK_I, the crack cannot be fully arrested, whereas crack growth rate is still reduced. In this regime, fatigue life of the specimen with healing capsules approaches the time for the healing agent to gel. As depicted by curve e in Figure 12, where ΔK_I = 0.529 MPa $m^{1/2}$ (K_{max}/K_{IC} = 0.81), the crack growth is retarded at the beginning in a way similar to curve f in Figure 11. Following this period of crack arrest, the crack eventually grows past the healed precrack at ~7×10^4 cycles. The subsequent crack growth behavior is a combination of steady growth and retardation, offering a healing efficiency of about 1335%. In the course of fatigue crack propagation, as shown in the Supporting Information, Figure S2g,h, a large quantity of epoxy healing agent was squeezed into thin cakes densely covering the fatigue fracture surface. Cohesive failure of the cured healing agent membranes contributes to retardation of crack growth. Adhesive bonding mechanism governs fatigue life extension in this regime.

When ΔK_I is further increased, crack growth is gradually sped up. As shown by curve d in Figure 11, where ΔK_I = 0.554 MPa $m^{1/2}$ (K_{max}/K_{IC} = 0.85), the crack growth is also retarded at the beginning similar to the case of curve e in Figure 11. Afterward, the crack grows past the healed precrack at ~5×10^4 cycles. The dependence of crack length on fatigue cycle is characterized by a combination of steady growth and retardation of crack, with a healing efficiency of about 566%. Cohesive failure of the cured healing agent membranes (see the Supporting Information, Figure S2e,f) implies that adhesive bonding mechanism is involved during the crack propagation.

As for high ΔK_I (i.e., when K_{max} approaches K_{IC}), mechanical kinetics of fatigue crack growth is extremely fast and the healing system does not have sufficient time to inhibit the crack propagation. This causes rapid failure of the specimen. As shown by curve c in Figure 11, where ΔK_I = 0.605 MPa $m^{1/2}$ (K_{max}/K_{IC} = 0.93), the fatigue crack in the specimen with healing capsules shows a constant growth rate with occasional crack retardation. Because the specimen fatigue life lags behind the time for the healing agent to gel, the healing efficiency has to be only 84%. Accordingly, the released healing agent has relatively sparsely covered the fatigue fracture surface, and some were stretched into tapeworm-shaped gels with obvious tearing traces (see the Supporting Information, Figure S2c, d). It suggests that the healing agent suffered from severe tension in the process of gelling or polymerization.

Figure 12 summarizes the dependence of life extension on ΔK_I. It is found that lower applied range of stress intensity corresponds to more evident retardation effect and higher healing efficiency. The result agrees well with that of specimens containing healing capsules without being exposed to high temperature.[23,28] In other words, the exposure of the composite at 200 °C for 12 h does not affect its capability for self-healing fatigue crack.

3.4. Effect of Higher-Temperature Curing on Healing Ability Studied by Monotonic Fracture Tests. The self-healing epoxy composites used for heat resistance evaluation in the above were first cured by room temperature curing system, and then heated to a certain temperature for a period of time. The findings help to understand healing ability of the composites operating under wider temperature range (50−250 °C), but it is still uncertain whether the healing agent can survive elevated temperature processing required by fabrication of advanced composites.

In this context, the present subsection is focused on the investigation of healing function of self-healing epoxy composites cured by medium temperature curing system (i.e., 2E4MIm) and high temperature curing system (i.e., DDS), respectively (refer to Experimental Section). Meanwhile, the embedded EPON 828-loaded microcapsules and hardener (mixture of PMP and DMP-30)-loaded microcapsules are the same as those employed hereinbefore.

Similar to the composites cured by room-temperature curing system, the results of fracture toughness tests show that the addition of 20 wt % microcapsules (i.e., 10 wt % epoxy-loaded microcapsules and 10 wt % hardener-loaded microcapsules) also increases the virgin monotonic fracture toughness of the epoxy cured by higher-temperature curing systems. In the case of 2E4MIm curing agent, K_{IC} is raised from 0.485 MPa $m^{1/2}$ of unfilled epoxy to 0.667 MPa $m^{1/2}$ of the filled version. As for DDS curing agent, K_{IC} of unfilled epoxy is 0.784 MPa $m^{1/2}$, whereas that of filled version is 1.061 MPa $m^{1/2}$. The relative

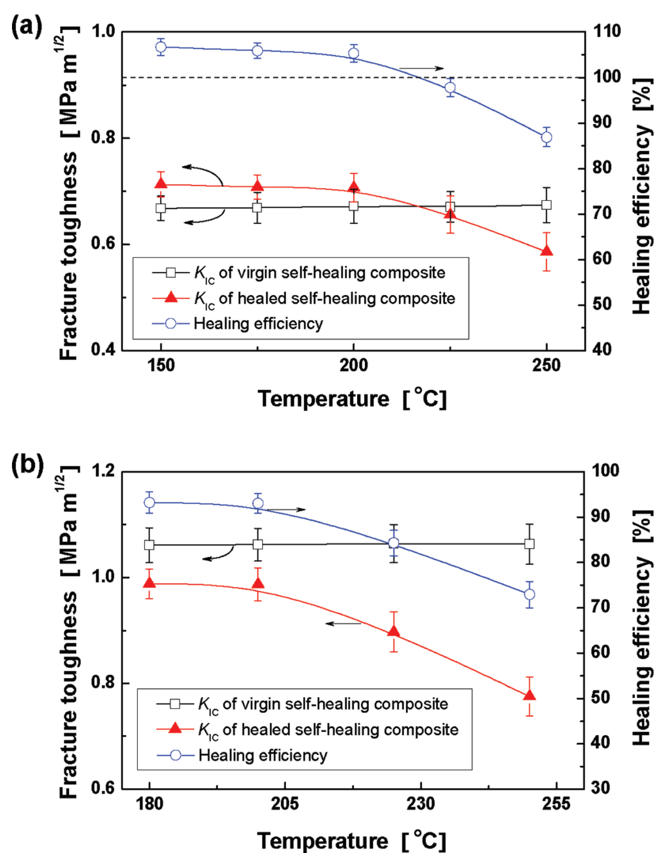

Figure 13. Influence of thermal exposure temperature on healing efficiency. The specimens with healing capsules were made from (a) medium- and (b) high-temperature curing systems, respectively. They were first exposed to different temperatures for 24 h. Having been placed at room temperature for more than 24 h, they were measured by the standard fracture toughness test procedure. Healing of the fractured specimens was conducted at room temperature for 24 h.

increments are 37.5 and 35.3%, respectively. More importantly, healing efficiency attains 106.8% for 2E4MIm cured system and 93.2% for DDS cured system (healing condition: room temperature, 24 h). Evidently, the healing agent has kept its capability during the composites manufacturing.

Figure 13 illustrates the influences of high temperature exposure (150−250 °C) on healing efficiency of 2E4MIm and DDS cured specimens. The specimens with healing capsules were first exposed to different temperatures for 24 h. Having been placed at room temperature for over 24 h, they were measured by the standard fracture toughness test. It is seen that fracture toughness of virgin composites is nearly independent of the exposure temperature at no higher than 250 °C, whereas that of healed composites starts to decrease when the exposure temperature is higher than 200 °C. As a result, the healing efficiency obviously decreases above 200 °C due to the deterioration of healing agent as previously discussed. The values corresponding to the exposure at 250 °C are 86.9 and 72.9% for 2E4MIm and DDS cured specimens, respectively. It suggests that below the ceiling value of 200 °C reactivity of the present healing agent is not affected by high temperature processing during composites manufacturing and high temperature exposure during application.

4. CONCLUSIONS

By replacing diglycidyl tetrahydro-o-phthalate and benzyl dimethylamine in the epoxy/mercaptan based healing system, which was previously developed by the authors,[19−21] with diglycidyl ether of bisphenol A and 2,4,6-tris(dimethylaminomethyl)phenol, heat resistance of the healing agent and self-healing epoxy composites is greatly improved. 200 °C represents the critical point for the present healing system. Below this temperature, self-healing ability of the composites remains at high level, no matter whether the composites are cured by high temperature curing agent or exposed to high temperature environment. Even when the exposure temperature is as high as 250 °C, moreover, healing efficiency of the composites can be about 72−86%, depending upon processing conditions.

On the basis of the present research, heat resistance of the present healing agent is expected to be further raised by using (i) chemicals with much higher thermal stability like fluorinated diglycidyl ether of bisphenol as the polymerizable resin and imidazole compounds as the catalyst and (ii) more advanced microencapsulation technology with inorganic substance as the wall.

ASSOCIATED CONTENT

Supporting Information. Representative SEM images of monotonic and fatigue fracture surfaces. This material is available free of charge via the Internet at http://pubs.acs.org.

AUTHOR INFORMATION

Corresponding Author

*E-mail: ceszmq@mail.sysu.edu.cn. Phone & fax: +86-20-84114008.

ACKNOWLEDGMENT

The authors are grateful to the support of the Natural Science Foundation of China (Grants U0634001, 50903095, 20874117, 50573093 and 51073176), Doctoral Fund of the Ministry of Education of China (Grant 20090171110026), the Science and Technology Program of Guangdong Province (Grant 2010B-010800021), and China Postdoctoral Science Foundation and the Fundamental Research Funds for the Central Universities.

REFERENCES

(1) Mauldin, T. C.; Kessler, M. R. *Int. Mater. Rev.* **2010**, *55*, 317–346.
(2) Blaiszik, B. J.; Kramer, S. L. B.; Olugebefola, S. C.; Moore, J. S.; Sottos, N.; White, S. R. *Annu. Rev. Mater. Res.* **2010**, *40*, 179–211.
(3) Yuan, Y. C.; Yin, T.; Rong, M. Z.; Zhang, M. Q. *Express Polym. Lett.* **2008**, *2*, 238–250.
(4) White, S. R.; Sottos, N. R.; Geubelle, P. H.; Moore, J. S.; Kessler, M. R.; Sriram, S. R.; Brown, E. N.; Viswanathan, S. *Nature* **2001**, *409*, 794–797.
(5) Trask, R. S.; Williams, G. J.; Bond, I. P. *J. R. Soc. Interface* **2007**, *4*, 363–371.
(6) Jones, F. R.; Hayes, S. A.; Zhang, W. *J. R. Soc. Interface* **2007**, *4*, 381–387.
(7) Xiao, D. S.; Yuan, Y. C.; Rong, M. Z.; Zhang, M. Q. *Adv. Funct. Mater.* **2009**, *19*, 2289–2296.
(8) Xiao, D. S.; Yuan, Y. C.; Rong, M. Z.; Zhang, M. Q. *Polymer* **2009**, *50*, 2967–2975.
(9) Lee, J.; Bhattacharyya, D.; Zhang, M. Q.; Yuan, Y. C. *Express Polym. Lett.* **2011**, *5* (3), 246–253.
(10) Yao, L.; Rong, M. Z.; Zhang, M. Q.; Yuan, Y. C. *J. Mater. Chem.* **2011**, *21*, 9060–9065.

(11) Wang, H. P.; Yuan, Y. C.; Rong, M. Z.; Zhang, M. Q. *Macromolecules* **2010**, *43*, 595–598.

(12) Meng, L. M.; Yuan, Y. C.; Rong, M. Z.; Zhang, M. Q. *J. Mater. Chem.* **2010**, *20*, 6030–6038.

(13) Yin, T.; Rong, M. Z.; Zhang, M. Q.; Yang, G. C. *Compos. Sci. Technol.* **2007**, *67*, 201–212.

(14) Yin, T.; Zhou, L.; Rong, M. Z.; Zhang, M. Q. *Smart Mater. Struct.* **2008**, *17*, 015019.

(15) Yin, T.; Rong, M. Z.; Wu, J. S.; Chen, H. B.; Zhang, M. Q. *Composites, Part A* **2009**, *39*, 1479–1487.

(16) Yin, T.; Rong, M. Z.; Zhang, M. Q.; Zhao, J. Q. *Smart Mater. Struct.* **2009**, *18*, 074001.

(17) Mangun, C. L.; Mader, A. C.; Sottos, N. R.; White, S. R. *Polymer* **2010**, *51*, 4063–4068.

(18) Jin, H.; Mangun, C. L.; Stradley, D. S.; Sottos, N. R.; White, S. R. In *Proceedings of the 3rd International Conference on Self-Healing Materials*; Bath, U.K., June 27−29, 2011; University of Bristol: Bristol, U.K., 2011; pp 269−270.

(19) Yuan, Y. C.; Rong, M. Z.; Zhang, M. Q.; Chen, J.; Yang, G. C.; Li, X. M. *Macromolecules* **2008**, *41*, 5197–5202.

(20) Yuan, Y. C.; Rong, M. Z.; Zhang, M. Q.; Yang, G. C. *Polymer* **2009**, *50*, 5771–5781.

(21) Yuan, Y. C.; He, Y. P.; Rong, M. Z.; Wu, J. S.; Zhang, M. Q.; Qin, S. X.; Yang, G. C.; Zhao, J. Q. *Smart Mater. Struct.* **2011**, *20*, 015024.

(22) Brown, E. N.; Sottos, N. R.; White, S. R. *Exp. Mech.* **2002**, *42*, 372–379.

(23) Yuan, Y. C.; Rong, M. Z.; Zhang, M. Q.; Yang, G. C.; Zhao, J. Q. *Express Polym. Lett.* **2011**, *5*, 47–59.

(24) Brown, E. N.; White, S. R.; Sottos, N. R. *Compos. Sci. Technol.* **2005**, *65*, 2474–2480.

(25) Jones, A. S.; Rule, J. D.; Moore, J. S.; Sottos, N. R.; White, S. R. *J. R. Soc. Interface* **2007**, *4*, 395–403.

(26) Dietrich, K.; Bonatz, E.; Nastke, R.; Herma, H.; Walter, M.; Teige, W. *Acta Polym.* **1990**, *41*, 91–95.

(27) Brown, E. N.; White, S. R.; Sottos, N. R. *J. Mater. Sci.* **2004**, *39*, 1703–1710.

(28) Yuan, Y. C.; Rong, M. Z.; Zhang, M. Q.; Yang, G. C.; Zhao, J. Q. *Express Polym. Lett.* **2010**, *4*, 644–658.